THE BEAM LOSS MONITORING SYSTEM

B. Dehning, G. Ferioli, J.L. Gonzalez, G. Guaglio, E.B. Holzer, C. Zamantzas,
CERN, Geneva, Switzerland

Abstract

The ionisation chamber and secondary emission based beam loss observation system will be used to optimise the accelerator tuning and to prevent the occurrence of magnet quenches and damages. For quench prevention and damage protection, a calibration of the system is needed in respect to the quench and damage levels of the magnets. The calibration of the system is based on tertiary beam halo tracking and on lost proton initiated shower simulations. Some of the calculated calibration constants should be verified during the foreseen sector test. The change of the thresholds, due to loss duration and beam energy, has to be tested during the commissioning phase of the LHC. The variation of calibration values at the location of the detectors, due to variations of the beam parameters, are planed to be addressed by tracking simulations, which will result in a calibration value spread. First particle tracking results show that loss locations in the arc region occur as expected at the quadrupole magnets. In the dispersion suppressor, behind the IP7 collimation, unexpected loss locations are observed at the bending magnets. The variations due to monitor internal parameter changes, at the lower limit of the dynamic range, are compensated by an internal measurement and test system. These automatic tests are foreseen during the times without beam. The resolution limit of the monitoring system has not been determined exactly yet. The tests are also needed to reach the required value of the mean time between failures for the monitor system. In the region of the dump levels only negligible variations are expected from the monitoring system itself. The variations from the beam parameter changes are expected to be dominant. Secondary shower simulation of the collimation in IP3 show that all BLM signals are largely dominated by the secondary shower signals originating from further upstream monitors, except for the first BLM downstream of the primary collimator.

INTRODUCTION

The commissioning and running in aspects of the BLM system will be discussed and motivated by the features of the system. Two aspects are of interest: the system features in the operational region of the dump levels and the behaviour of the system at the lower end of the dynamic range (resolution). The dump level features are most interesting to allow a reliable protection of the magnets by the generation of a dump signal. The low end dynamic range features will determine the resolution of the system and therefore the machine tuning possibilities. This feature will have an influence on the needed beam time to optimise the loss amplitudes and the loss locations.

These considerations are only valid for the non collimation area beam loss monitoring system. Since the loss rates in the collimation areas are several orders of magnitude higher than in the straight and arc locations, and as the loss locations (collimators) are only meters apart, the system features are very different. Some of the measurement system features will be discussed at the end.

SYSTEM LAYOUT

The majority of the detectors of the BLM system will be ionisation chambers and, for regions with very high loss rates, secondary emission monitors (SEM) are foreseen as well. The ionisation chamber consists of a stack of parallel electrodes, which is inserted in a stainless steel tube (see Fig. 1). The volume of the chamber is filled with gas (N_2 in the SPS) under normal pressure. The electrical field strength in between of the electrodes is 3 kV/cm. The only passive electronic components are a resistor and a capacitor of a low pass filter mounted at the feedthroughs of the chambers. This filter smoothes drift voltage variations and, in the case of a break down of the voltage power supply, it keeps the drift voltage almost constant at the electrodes of the chamber. The correct functioning of the ionisation chamber is therefore insured for minutes after switch off, even in case of a break down.

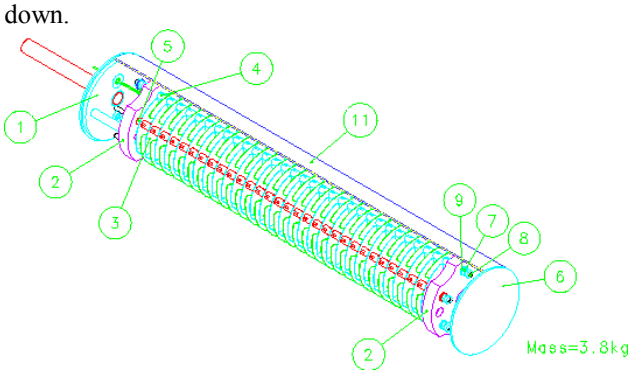

Figure 1: Drawing of the LHC ionisation chamber (diameter 89mm, length 500 mm, active volume 1.5 l).

The SEM detector will be based on the same design as the ionisation chamber. Instead of having the electrode volume filled with a gas it will be under vacuum and only one sensitive foil will be used to reduce the resolution (see Fig. 2, left foil of number 3). It is foreseen to have

one tube shape assemble with a short SEM part on one side and a longer ionisation chamber part on the other side.

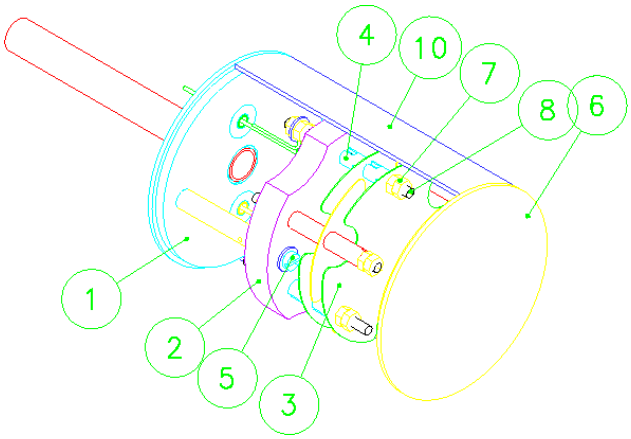

Figure 2: Drawing of the secondary emission monitor (diameter 89 mm, length 100 mm).

Both detectors will be mounted on the outside of the cryostat in the horizontal plane given by the two vacuum pipes of the LHC magnets (see Fig. 3). At this position the secondary particle flux is highest and the best separation of the losses from the two beams is reached.

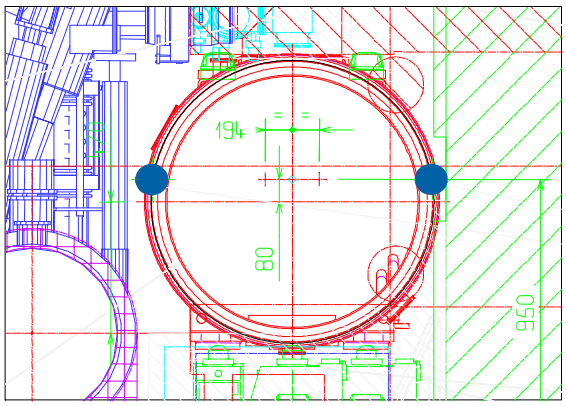

Figure 3: Cross section drawing of the LHC tunnel with the cryo line and the cryostat of a quadrupole magnet. The beam loss detectors are indicated by the two blue circles in the plane of the vacuum chambers.

The electrical signals of the detectors are digitised with a current to frequency converter. It is located below the quadrupole magnet in the arc and elsewhere in the RR and UJ location for all detectors of the dispersion suppressor and the long straight sections (see Fig. 4). The analog signal transmission cables have a length of a few meters (arc), up to 300 m (long straight section). This part of the transmission is subject to the injection of electromagnetic cross talk and noise. It is foreseen to use the same electronics for the two detector system. The further discussions will concentrate only on the ionisation chamber based signal generation and treatment, because this design is more advanced.

PERFORMANCE AT DUMP LEVELS

To evaluate the feature of the system in the region of the dump levels the detector currents are shown in table 1. The minimum quench level currents for 450 GeV beam and 7 TeV, are 2 to 12.5 nA respectively. The specified relative reproducibility for the dump levels is 0.25. The aimed reproducibility value for the system in the dump level region is 0.05.

Table 1: Detector currents of a 1 litre ionisation chamber at different regions of the operational range.

450 GeV, quench levels (min)	100 s	12.5 nA
7 TeV, quench levels (min)	100 s	2 nA
Required 25 % rel. accuracy, error small against 25% => 5 %		100 pA
450 GeV, dynamic range min.	10	10 pA
	100	2.5 pA
7 TeV, dynamic range min.	10 s	160 pA
	100s	80 pA

The expected systematic errors of the system at quench

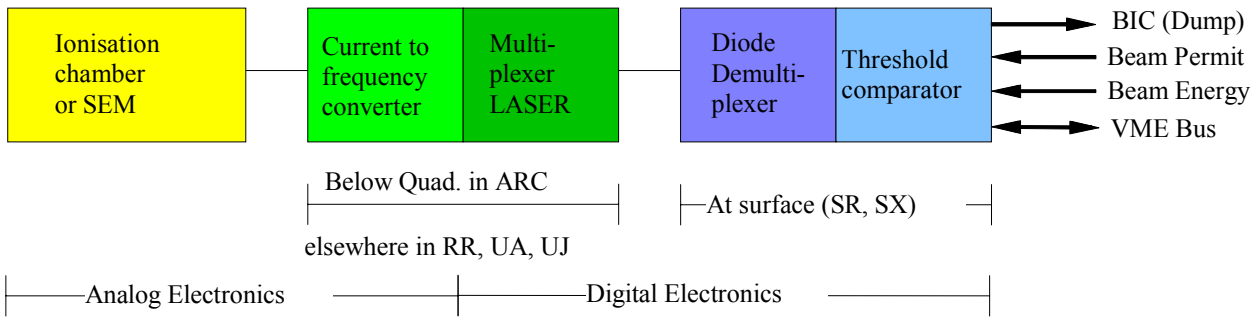

Figure 4: Schematic view of the BLM detector and signal transmission chain

levels are listed in table 2. The largest errors are given by the approximation of the dump levels and probably by the topology of the losses. Most uncertainties are systematic errors, which will allow compensation after a calibration procedure. In the third column of table 2 the means are listed, which should allow a determination of the errors.

The detector uncertainty is originating from uncertainties in the simulation code and should be eliminated by calibration measurements. These measurements should be done before the installation of the detectors in the LHC, with sources and test beams.

The radiation single event effect is caused by the passage of charged particles through the components at the input of the analog electronics. This effect is largest in the arc, since the electronics is located below the quadrupole magnets. The effect is proportional to the loss rate and scaled down by the lower fluence at the location of the current to frequency converter, compared to the location of the detectors (phi dependence of the fluence distribution: almost a factor 10) [1].

Table 2: Expected systematic errors of the system in the region of the quench levels.

	relative accuracies	Correction means
Electronics	< 10 %	Electronic calibration
Detector	< 10 – 20 %	Source/sim./measurements
Radiation – SEE	about 1 %	
fluence per proton	< 10 - 30 %	sim. / measurements with beam (sector test)
Quench levels (sim.)	< 200 %	measurements with beam (sector test) / scaling
Topology of losses (sim.)	< large	sim. / measurements

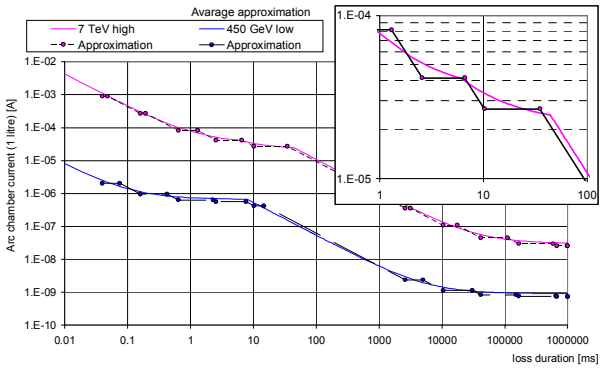

Figure 5: The quench level dependence as function of loss duration. The zoomed curve shows the quench level curve and the approximation function.

The electronics uncertainties are mainly given by the dump level approximation procedure (see Fig. 5).

The approximation accuracy can be optimised by changing the number of curve supporting values and by introducing non equidistant curve supports. This procedure will be used for the loss level variation with time and for the loss level variation with the beam energy. Two dimensional tables will be created and loaded, in non volatile RAM, on the threshold comparator card. The table could be different for every beam loss monitor channel. The approximation error will be kept negligible compared to other errors of the monitoring system.

The secondary particle flux at the location of the detectors, normalised to the number of inducing protons is called the fluence. In figure 6 an example is shown for the

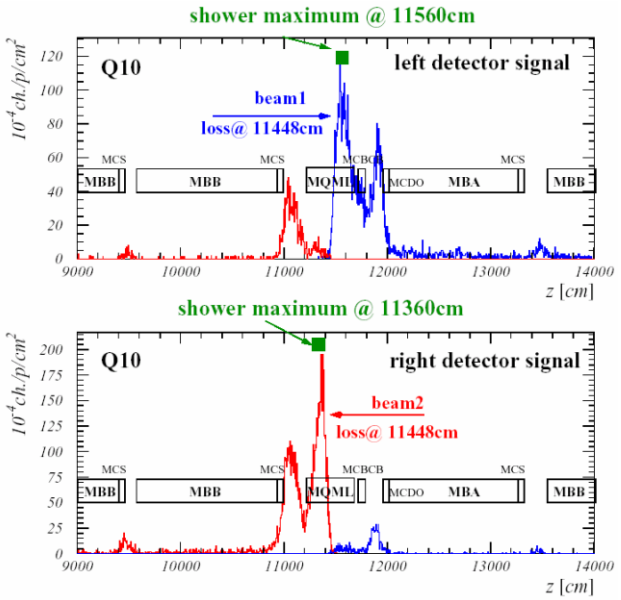

Figure 6: Fluence distribution along dispersion suppressor magnets. The proton impact is in the centre of the quadrupole magnet for both beams.

fluence along the magnets (MB, MQ, MB) with a proton impact at the centre of the MQ magnet. The uncertainty of this simulation is mainly determined by uncertainties in the shower developments and in the knowledge of the geometry. It is expected that this is a systematic effect which could be calibrated.

The uncertainties in the topology of the losses are expected to be of statistical and systematic nature. First simulations show that the losses in the arc occur at the expected locations at the quadrupole magnets (see Fig. 7) [3]. The fluctuations of loss amplitudes and especially the variation of the locations of the highest power depositions in the magnets are not simulated yet.

In the dispersion suppressor after the collimation area IP7 the loss location are not only concentrated at the quadrupole magnets (see Fig.8). The losses are almost dispersed distributed along all magnets. These loss

patterns are not anticipated by the definition of the location of the beam loss monitors yet. In addition of

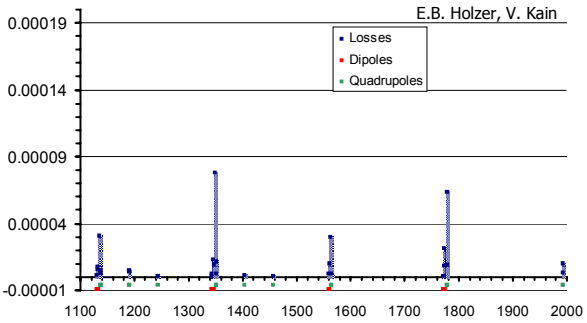

Figure 7: Relative distributions of proton losses in the LHC arc between IP7 and IP8 (bin width 1m).

these loss patterns the magnitude, of the variations is not simulated yet.

At the dispersion suppressor, after the collimation area, not only losses from the tertiary halo are expected, but in

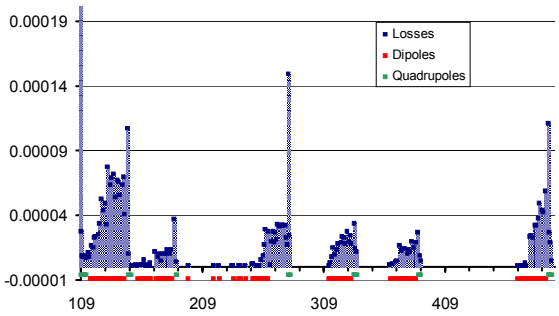

Figure 8: Relative loss distribution in the dispersion suppressor after the collimation area in IP7 in the direction to IP8 (bin width 1m).

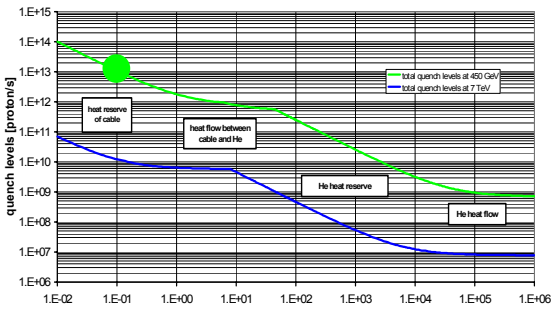

Figure 9: The quench level rate as function of the loss duration. The green dot indicates the location where a comparison between simulations and measurements would be possible.

addition a large contribution is expected from the secondary shower particles, which are created in the collimators and the surrounding materials. The shower simulations for these contributions to the particle impact on the vacuum chamber have not yet been done.

The sector test will allow the checking of some simulations, if the proton beam is directed onto the vacuum chamber. It should be possible to measure the relative distribution of the particle fluence with several detectors positioned along the magnets, even without knowing the exact impact position of the proton beam. These measurements will result in a check of the fluence simulation for this magnet configuration. A check of the quench level simulations is only possible for one beam energy and for one loss duration (see Fig.9).

These measurements will result in a check of the secondary shower induced heat into the cable and in the check of the heat capacity of the super conducting cable. An overall scaling of the quench level curve will be possible.

As shown in table 2 the largest uncertainties of the BLM system are expected to be related to the topology of the loss and the quench level knowledge. It is foreseen that uncertainties of the detector and the electronics are minimised before the start up. Lab tests of the electronics, radioactive source tests of the detector and electrical tests of the installed system should insure a reliable measurement of the secondary particle flux. It is expected that further simulations of the loss topology will result in a better understanding of this source of uncertainties.

PERFORMANCE AT THE LOW LIMIT OF THE DYNAMIC RANGE

At the limit of the dynamic range the performance will be dominated by noise sources and by the behaviour of the input elements of the current to frequency converter. The low limit input currents range from 2.5 pA, at 450 GeV, to 80 pA, at 7 TeV (see Tab. 1). The sources of variations and their presently uncorrected magnitude are listed in table 3.

Table 3: Sources of dark current changes.

Radiation: (Iafter - Ibefore) @ 500 Gy	Linear increase	+50 pA
Temperature: (6 days, assumed temp. variation 2 degree)	at 1 n A Non radiated channel / Radiated channel	+-27/-83 pA
Humidity	To be done	
Radioactive activation 450 GeV / 7 TeV	1e-2 to 1e-4 (SPS 1e-3)	1.2 – 120 pA /0.02 - 2 pA
EMC noise for long cable	ongoing	

The radiation sensitivity was tested for each component at the input stage of the current to frequency converter. Two components cause a drift of the input dark current. The JFET based switch increases the current by 70 pA and the FET input of the operational amplifier decreases the current by 20 pA. In table 3 they are combined to a current increase by 50 pA. The temperature dependence of the current to frequency converter is still under study. Preliminary measurements indicate that, due to radiation exposure, the temperature dependence increases by a factor 3 to 4. The temperature dependence and the humidity dependence will be studied in detail.

Another concern is the electromagnetic noise introduced in the analog part of the signal chain. It is expected that the arc monitor system is not significantly concerned, due to the short distance between detectors and the digitalisation by the current to frequency converter. The other foreseen installations in the long straight section and the dispersion suppressor, will be tested with an equivalent set up in SPS before the final design.

The activation of the materials around the chamber and of the chamber materials themselves, will contribute to the chamber signal. This effect will scale with the average particle flux. Preliminary estimates indicate that the ratio between average particle flux and activation rate will vary between $1x10^{-4}$ to $1x10^{-2}$ [2]. This effect needs a more precise simulation based estimate, especially for the detectors in the collimation area.

To overcome input dark current variations it is foreseen to make a measurement in between of two LHC fills. This value will be recorded and checked for consistency and automatically subtracted from the measurements during the fill. In addition it is foreseen to modulate the drift voltage power supply of the ionisation chambers. With this procedure different elements will be checked:

- The components in the ionisation chamber (R, C)
- The capacity of the chamber (insulation)
- The cable connection
- The stable signal between few pA to some nA (quench level region).

The only remaining non surveyed element, is the gas gain of the ionisation chamber. It is not possible to use any method which is based on electrical test signal measurements. Therefore the only possible check is based on a signal generation using a radioactive source. This time consuming procedure could only be applied during times with no beam. Based on the experience from the usage of ionisation chambers in SPS, a significant mal functioning is not expected in 20 years for detectors outside the collimation areas.

The ionisation chambers in the SPS were tested after over 20 years of operation using a Cs source. The source was placed on the mounted chambers and the signals were read out with the standard installed BLM electronics of the SPS (see Fig. 10).

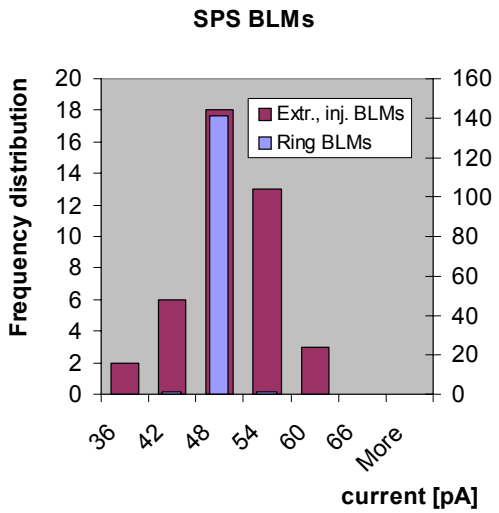

Figure 10: Distribution of the SPS ionisation chamber currents created with a caesium source.

The measurements were grouped in two sets, one included the measurements from the chambers in the ring and the other set the chambers from the injection and extraction areas of the SPS. Almost all ring chambers (141 out of 143) fall into a bin with a width of 6 pA and the others are distributed over five bins. The two locations differ by the amount of the radiation dose received. The

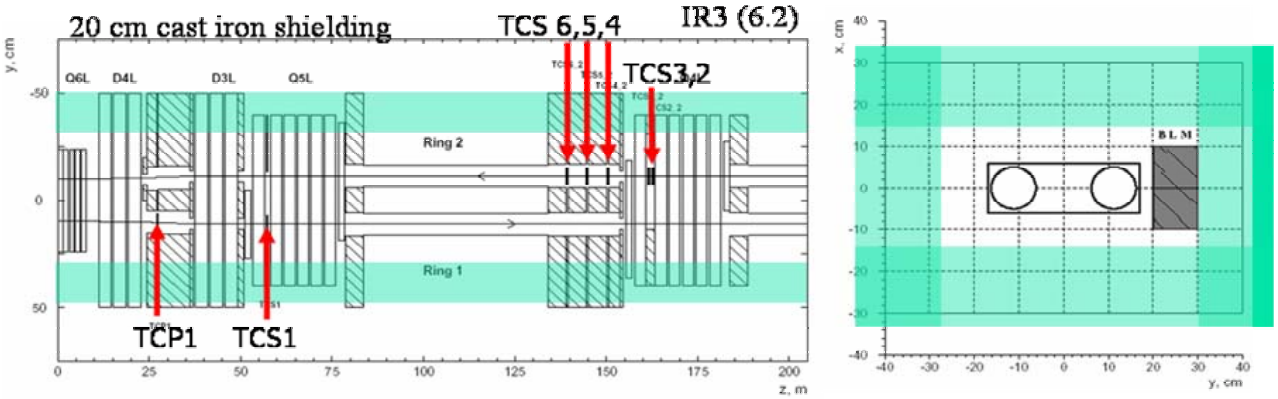

Figure 11: Layout of the momentum collimation area in IP3 (only one side of the IP is drawn, the other side is point symmetric). The green bars indicate the foreseen cast iron shielding.

influence of the radiation caused a gain variation of up to 30 %. It is assumed that the SPS dose values exceed the expected dose for the LHC non collimation areas by orders of magnitudes. A more quantitative doses estimate received by the SPS chambers will be done.

BEAM LOSS MEASURENTS IN THE COLLIMATION AREAS

It is foreseen to locate a beam loss monitor behind every collimator. The layout of the momentum collimation in IP3 was chosen to study the loss signals on a less complex system compared to the betatron cleaning in IP7 [4]. The proton impact distribution for each collimator was used to create secondary particle showers, which could be measured by detecting ionising particles near the collimators.

The used optics was version 6.2 with the primary (TCP) and the secondary collimators (TCS), consisting of double density carbon. The lengths of the collimators are 0.20 m (TCP) and 0.50 m (TCS). The primary collimator is located between the bending magnets, D4 and D3, and the first secondary collimator about 30 meters downstream, just in front of Q5 (see Fig. 11). The other secondary collimators are grouped on the other side of the

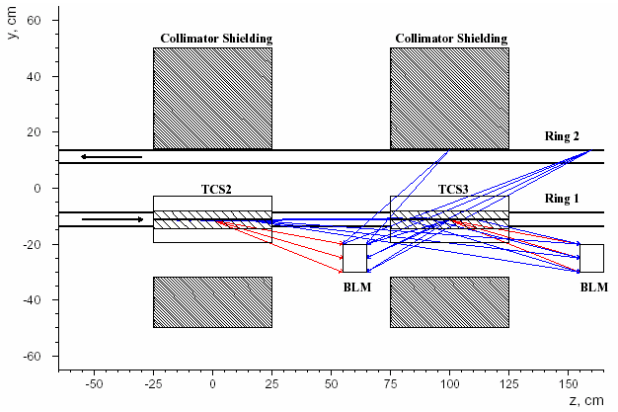

Figure 12: Detailed view of the collimator layout with all possible secondary particle shower sources indicated.

IP, about 200 m downstream of Q4. The foreseen position of the loss monitors are about 30 cm downstream of the collimators. The aim was to disentangle the different sources of the shower particles contributing to the particle signal at different transverse locations (see Fig. 12). The 2 D distribution is relatively flat over a square with corner length of 80 cm (see Fig. 13, top). The relative signal contribution in a BLM, monitor from the adjacent upstream collimator, is shown in figure 14. The upstream monitor (BLM 1) of the collimator TCP1 receives only secondary shower particles originating from interaction in TCP1. The situation is very different for all other monitors. The upstream monitor (BLM 2) of the collimator TCS 1 receives most of the secondary shower particles originating from interaction in TCP1 and only 4 % from the adjacent upstream collimator. The relative signal values from the other collimators are 57%, 9%, 5%, 4% and 1%. The larger "good" signal of BLM 3 is

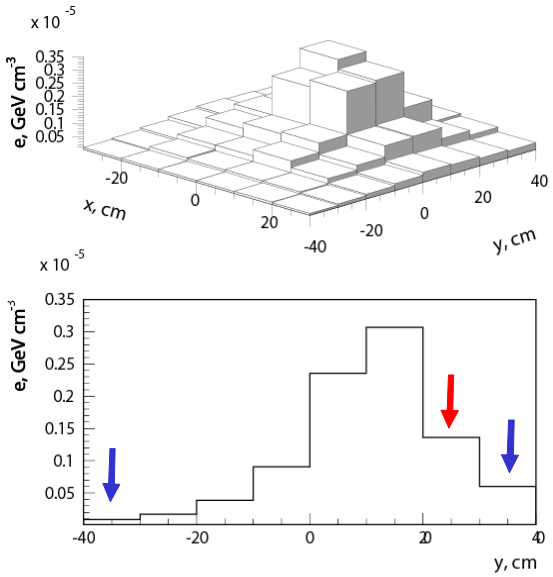

Figure 13: Top: 2D distribution of the energy deposition in a volume of one litre 30 cm. downstream of the collimator TCS1. Bottom: Horizontal slice at the vertical position between 0 and 10 cm.

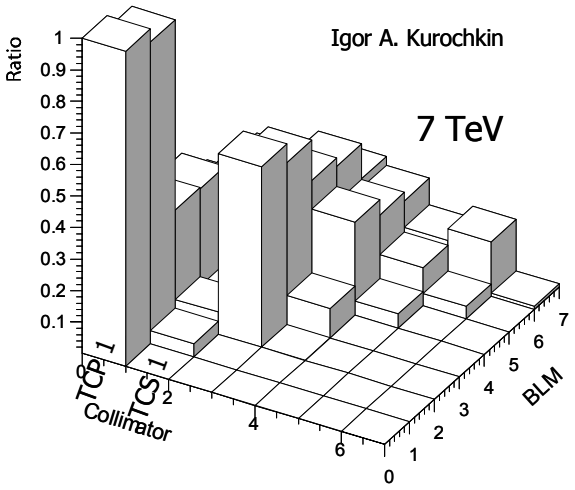

Figure 14: Relative signal in a beam loss monitor as function of the monitor and as function of the collimator number.

due to the large distance between TCS1 and TCS2 (200 m).

It was tried to improve the signal to cross talk value by moving the detector to two other locations at larger distances from the beam tube (see Fig. 13, bottom, blue arrows). The signal to noise ratio decreased even more

indicating that signal (shower particles originating from the nearest upstream monitor) diminishes faster than the cross talk contribution.

CONCLUSION

It is expected that quench prevention and damage protection uncertainties will depend mainly on quench level knowledge and the topology of loss variations, not on BLM calibrations or variations. The sector test will likely result in a calibration of the quench level for 450 GeV and for a loss duration of one turn. Quench level variations with an energy and 7 TeV levels have to be calibrated during LHC operation.

The low level signal variation will be partially compensated by an automatic test procedure, the remaining magnitude of variation will de determined.

The loss location and loss topology as well as variation need more simulations introducing realistic beam conditions.

The collimation loss detection system will be dominated by secondary particle background and the resolution of the detectors is likely to be spoiled by the activation of the surrounding materials. No improvements are expected to be possible, the only suggested approach is a combined beam, beam-halo, signal observation simulation.

ACKKNOWLEGDEMENTS

The authors would like to thank Verna Kain for providing the plots of the proton loss downstream of the collimation in IP7 and Igor Kurochkin for the plots of the secondary shower distributions in the collimation area of IP3.

REFERENCES

[1] Geschwendner E., et al.,"The Beam Loss Detection System of the LHC Ring, EPAC'02, Paris, June 2002, p. 1894.
[2] Brugger, M., private communication.
[3] Holzer E.B., Kain V., unpublished simulation studies.
[4] Kurotchkin I. A., et al., unpublished simulation studies.